Electronic Supplementary Information

Selective Capture and Rapid Identification of *E. coli* O157:H7 by Carbon Nanotubes Multilayer Biosensors and Microfluidic chip-based LAMP

*Tianchan Li, [a] Fanjiao Zhu,[a] Wei Guo,[a] Hongxi Gu,[a] Jing Zhao,[a] Mei Yan, *[ab] Shaoqin Liu*[ab]*

a School of Life Science and Technology, State Key Laboratory of Urban Water Resource and Environment, Harbin Institute of Technology, Harbin 150080, China

b Micro- and Nanotechnology Research Center, Harbin Institute of Technology, Harbin 150080, China

E-mail: yanmei@hit.edu.cn; shaoqinliu@hit.edu.cn

Part S1 Preparation, characterization and bacterial capture capability of the CNT multilayer biosensors
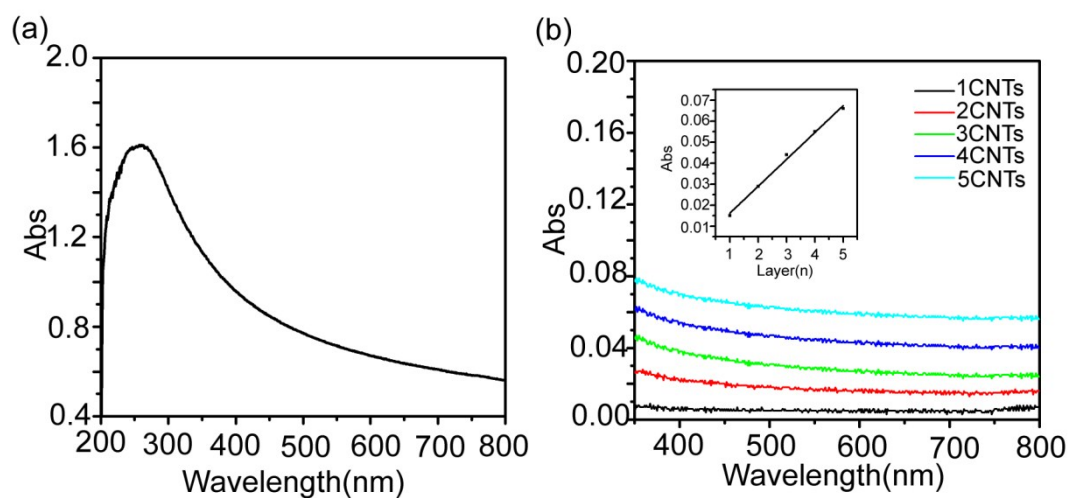
Fig. S1 (a) Absorption spectra of MWCNTs. (b) UV-vis spectra of (MWCNT/PEI)n multilayers assembled onto ITO electrode surface. In the range of 350-800 nm, the absorbance is gradually increased with the number of bilayers n. The inset shows the linear relationship between the absorbance at 400 nm and the MWCNT/PEI bilayer numbers, demonstrating that the LBL assembly process is reproducible, uniform and stable.
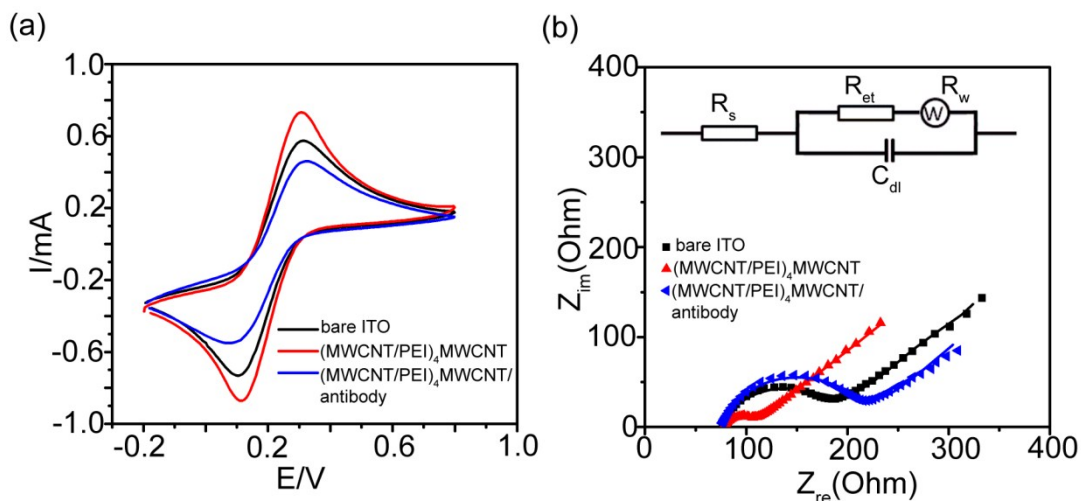
Fig. S2 Cyclic voltammograms (a) and EIS spectra (b) of $[Fe(CN)_6]^{3-/4-}$ at bare ITO electrode (black curve), $(MWCNT/PEI)_4MWCNT$ multilayers-coated ITO electode (red curve), and the anti-*E. coli* O157:H7 polyclonal antibody-modified $(MWCNT/PEI)_4MWCNT$ electrode (blue curve). The dot plots are real experiments results, while the line curves are fitting results using the inserted equivalent circuit, where R_s equals the resistance of solution, R_{et} is the charge transfer resistance, R_w represents Warburg resistance, and C_{dl} is double layer capacitance.

As shown in **Fig. S2a**, the $[Fe(CN)_6]^{3-/4-}$ redox probe exhibited a reversible behavior on the bare ITO electrode. The deposition of $(MWCNT/PEI)_4MWCNT$ multilayers onto ITO electrode resulted in the obvious increase in oxidation and reduction peak currents of $[Fe(CN)_6]^{3-/4-}$ probe. This increase can be explained in two reasons: (1) MWCNT has good conductivity, which facilitates electron transfer between the electrolyte and the ITO electrode; (2) The structure of MWCNT network in the multilayer film increase the electrochemically active area. After the nonconductive antibody layer attached to $(MWCNT/PEI)_4MWCNT$ multilayers through covalent bond, the antibody hampers the electron transfer of the redox probes, resulting in the decrease in peak current.

Electrochemical impedance spectroscopy (EIS) also confirmed the stepwise assembly of the bacterial biosensors. **Fig. S2b** illustrates the results of the Nyquist plot of the ITO electrode after each modification step. As shown in **Fig. S2b**, an

obvious semicircle was observed at high frequencies, corresponding to the electron transfer-limited process. A straight line with a slope close to unity appears at lower frequencies, resulting from the diffusion limiting of the redox species from the electrolyte to the electrode interface. The generated double layer capacitance (C_{dl}) and the charge transfer resistance (R_{et}) can be calculated from this spectrum using a simple equivalent circuit (the inset of **Fig. S2b**).[1] The R_{et} value of bare ITO electrode, (MWCNT/PEI)$_4$MWCNT multilayers-coated ITO electrode, and the anti-*E. coli* O157:H7 polyclonal antibody-modified (MWCNT/PEI)$_4$MWCNT electrode is about 75.12 Ω, 28.3±1.7 Ω and 127.13±3.12 Ω, respectively. This result demonstrates that the conductive CNT multilayers can dramatically enhance charge transfer of redox probes.
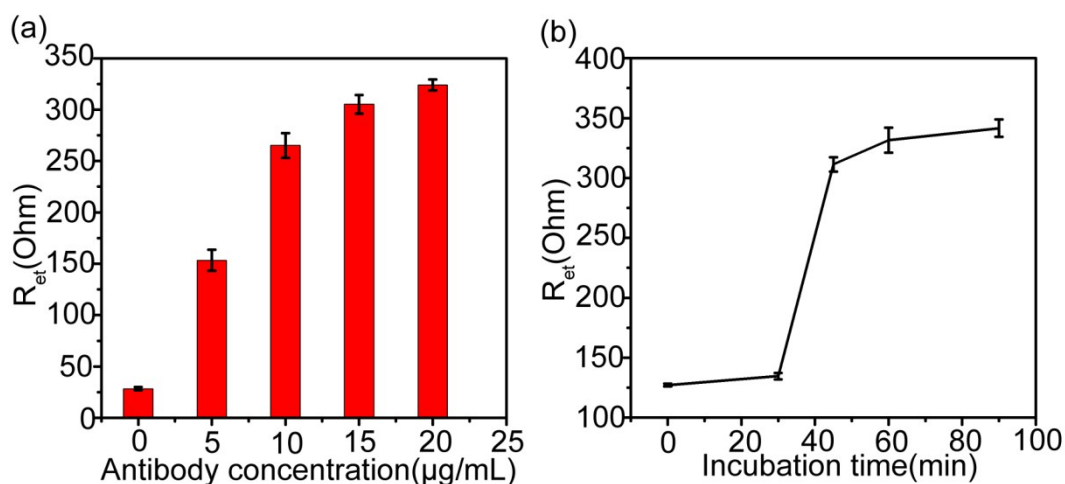
Fig. S3 (a) R_{et} of $(MWCNT/PEI)_4MWCNT/antibody$ modified ITO electrodes as a function of the antibody concentration. (b) R_{et} of $(MWCNT/PEI)_4MWCNT/antibody$ modified ITO electrodes as a function of the incubation time. The error bars represent the standard deviation of at least three measurements.

The influence of incubation time and antibody concentration during the functionalization process on *E. coli* O157:H7 capture efficiency was evaluated with EIS. As shown in **Fig. S3a**, in the range of 0-10 µg mL^{-1}, with the increasing of the concentration of antibody, an increase in the R_{et} value is observed due to the insulating properties of the bacteria attached on the electrode surface. Beyond a concentration of 10 µg mL^{-1}, the R_{et} value increases slowly, indicating that the electrode surface reached a saturation point at higher concentration. Next, we investigated the effect of the incubation time of the capture efficiency of *E. coli* O157:H7. The prepared sensors are exposed to 10^5 CFU per mL *E. coli* O157:H7 solution for 30, 45, 60 and 90 min, respectively. As shown in **Fig. S3b**, the R_{et} value increased with the increase of incubation time and reached equilibrium when the incubation time was 45 min. Based on above results, a suitable concentration of anti-*E. coli* O157:H7 polyclonal antibody was found to be 10 µg mL^{-1}. The optimal incubation time for the electrode was 45 min for the target capture.
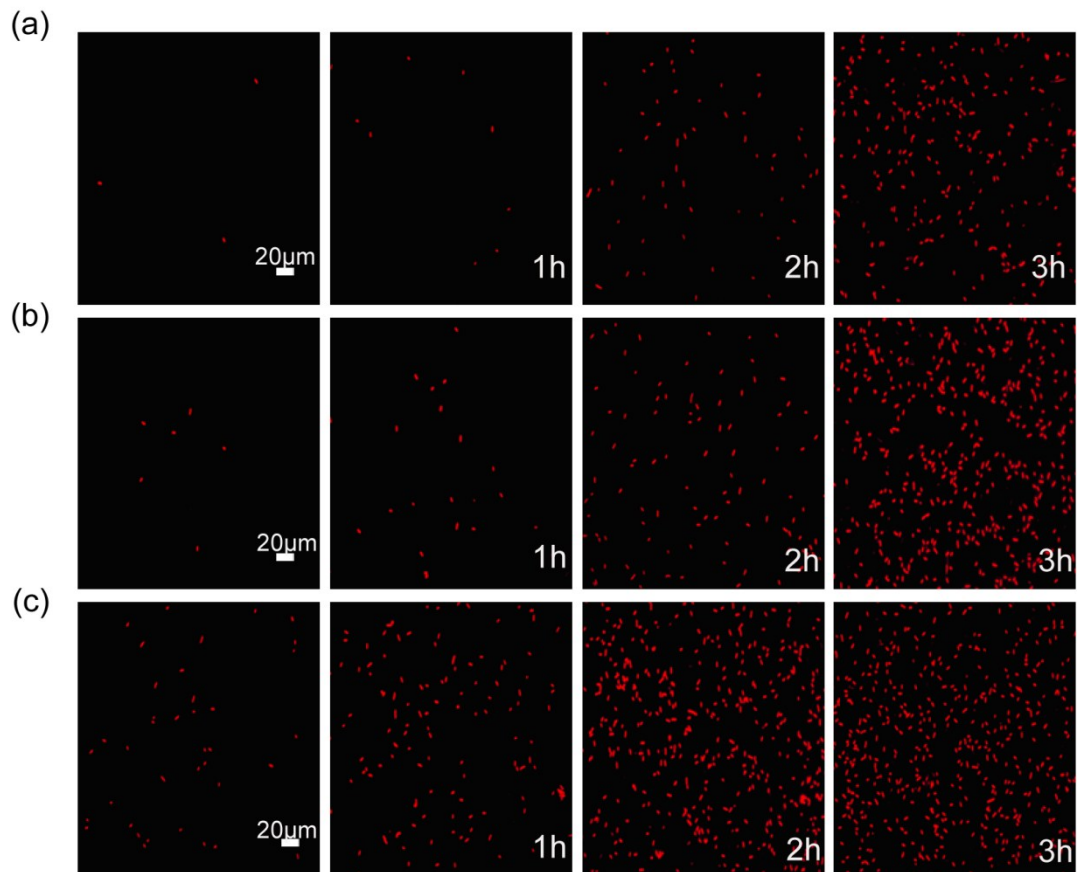
Fig. S4 Fluorescent images of different concentration of *E. coli* O157:H7 captured by the biochip before and after culturing for 1 h, 2 h, and 3 h, respectively. (a) 5 CFU mL^{-1}; (b) 10 CFU mL^{-1}; (c) 100 CFU mL^{-1}. Scale bars are 20 μm.

Part S2 Analytic performance of the combination microfluidic chip-based LAMP coupled with CNT multilayer biosensor

Table S1 Comparison of the proposed method and other *E. coli* O157:H7 sensors.

Detection method	LOD	Linear range	Reference
Electrochemical Detection	8.0×10^2 CFU mL^{-1}	1.0×10^3-1.0×10^7 CFU mL^{-1}	2
Chemiluminescence	10^3 CFU mL^{-1}		3
Chemiluminescence	1.2×10^3 CFU mL^{-1}	4.3×10^3-4.3×10^5 CFU mL^{-1}	4
An acoustophoresis chip-based PCR	10^3 CFU mL^{-1}		5
Real-time PCR	10^2 CFU mL^{-1}		6
microfluidic immunosensor	10^2 CFU mL$^{-1.}$		7
Impedimetric immunosensor	2 CFU mL^{-1}	30-3×10^4 CFU mL^{-1}	8
Impedimetric immunosensor	1.5×10^2 CFU mL^{-1}	1.5×10^2-1.5×10^7 CFU mL^{-1}	9
Impedimetric sensors	10^3 CFU mL^{-1}	10^3-10^7 CFU mL^{-1}.	10
Enzyme-linked immunosorbent assay	68 CFU mL^{-1}	6.8×10^2-6.8×10^3 CFU mL^{-1}	11
The proposed method	1 CFU mL^{-1}	1-10^4 CFU mL^{-1}	this study
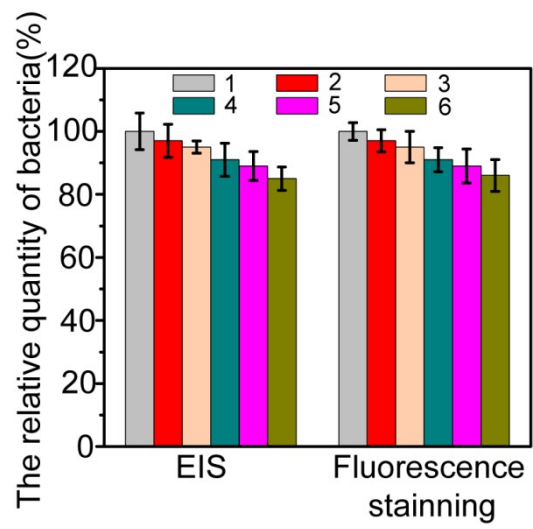
Fig. S5 Regeneration of the CNT multilayer biosensor. The concentration of *E. coli* O157:H7 is 50 CFU mL^{-1}.

Reference

1   C. Fernández-Sánchez, C. J. McNeil and K. Rawson, *Trends Anal. Chem.,* 2005, **24**, 37-48.

2   L. Xu, J. Du, Y. Deng and N. He, *J. Biomed. Nanotechnol.*, 2012, **8**, 1006-1011.

3   Z. Li, L. He, N. He, Z. Shi, H. Wang, S. Li, H. Liu, X. Li, Y. Dai and Z. Wang, *J. Nanosci. Nanotechno.*, 2010, **10**, 696-701.

4   Y. Zhang, C. Tan, R. Fei, X. Liu, Y. Zhou, J. Chen, H. Chen, R. Zhou and Y. Hu, *Anal. Chem.*, 2014, **86**, 1115-1122.

5   P. D. Ohlsson, M. Evander, K. Petersson, L. Mellhammar, A. Lehmusvuori, U. Karhunen, M. Soikkeli, T. Seppä, E. Tuunainen and A. Spangar, *Anal. Chem.*, 2016, **88**, 9403−9411.

6   Y. Liu and A. Mustapha, *Int. J. Food. Microbiol.*, 2014, **170**, 48-54.

7   F. Tan, P. H. Leung, Z.-b. Liu, Y. Zhang, L. Xiao, W. Ye, X. Zhang, L. Yi and M. Yang, *Sens. Actuators. B-Chem.*, 2011, **159**, 328-335.

8   M. B. dos Santos, J. Agusil, B. Prieto-Simón, C. Sporer, V. Teixeira and J. Samitier, *Biosens. Bioelectron.*, 2013, **45**, 174-180.

9   Y. Wang, J. Ping, Z. Ye, J. Wu and Y. Ying, *Biosens. Bioelectron.*, 2013, **49**, 492-498.

10 Y. Li, R. Afrasiabi, F. Fathi, N. Wang, C. Xiang, R. Love, Z. She and H.-B. Kraatz, *Biosens. Bioelectron.*, 2014, **58**, 193-199.

11 Z. Shen, N. Hou, M. Jin, Z. Qiu, J. Wang, B. Zhang, X. Wang, J. Wang, D. Zhou and J. Li, *Gut. Pathog.*, 2014, **6**, 14.